

Analysis of the Vibration Modes in the Diverter Switch of Load Tap Changer

Edwin Rivas

Universidad Distrital Francisco José de Caldas, Bogotá, Colombia

José Ignacio Rodríguez

Universidad Distrital Francisco José de Caldas, Bogotá, Colombia

Cesar Hernández

Universidad Distrital Francisco José de Caldas, Bogotá, Colombia

Copyright © 2017 Edwin Rivas, José Ignacio Rodríguez and Cesar Hernández. This article is distributed under the Creative Commons Attribution License, which permits unrestricted use, distribution, and reproduction in any medium, provided the original work is properly cited.

Abstract

In this article, the vibration modes of a load tap changer are analyzed along with their application coordinates their implication in the response of an experimental temporary signal acquired from the changer, the natural and resonance frequencies and the proportions in the displacements of the charger's commutator. They are simulated and analyzed with the finite element calculation software Algor™. The experimental data are obtained by measuring vibration signals in an on-load tap changer (OLTC) at the moment of changing taps; with a mono-axial accelerometer located over the vertical axis (head of the regulator). The acquired experimental data are analyzed with MATLAB™ software with the Wavelet discrete transform and the Fast Fourier Transform.

Keywords: CTC, selector, commutator, change of tap, frequencies, and vibration modes

1. Introduction

An on-load tap changer (OLTC) is the only part that moves in a transformer [1]. Its function is to perform the change operation from one tap to another in the regulation

winding. It is a response mechanism to a voltage variation in the network due to load variations. The OLTC keeps the transformer's output voltage constant by modifying the number of spirals in one of the windings without interrupting the load's current.

The OLTC is submitted to mechanical efforts and important electrical events. Hence, the OLTC is one of the transformer elements with the highest failure index: according to an international poll [2], 40% of the failures in a transformer are produced in the CTC.

The state of some elements of the changer (commutation resistances, contacts, etc.) can be evaluated with periodical inspections. However, these inspections require that the transformer is discharged, i.e. out of service for a relatively long time. This supposes a considerable expense and hiring qualified technicians and operators. Additionally, some of the parts of an OLTC (contacts, pre-selector, etc.) cannot be inspected due to their location within the transformer's tank.

The purpose of this work is to implement a methodology to determine the range of frequencies where a commutator's contacts should be when they are in good shape. Hence, the vibration modes of an OLTC have been correlated with the vibration frequencies coming from real signals of an operational OLTC.

The OLTC was implemented by modeling the commutator and performing simulations with the finite element calculation software Algor™ of commercial use. The real OLTC signals were processed with a Hilbert transform (envelope of the vibration signal) to then apply the Wavelet discrete transform.

With the purpose of determining diagnosis identifiers such as the number of vibration impulses, amplitude, time between impulses and frequency ranges where these impulses lie, the Fast Fourier transform was applied to the vibration signal in order to corroborate the frequency range. This work pretends to determine if the system's excitation frequency is very close to the OLTC's natural frequency since there could be a resonance phenomenon causing damages in the OLTC's structure and even collapse.

2. General Structure of an OLTC

A basic OLTC's structure (Figure 1) has these elements [3]:

1. Activation and control closet.
2. Transmission mechanism.
3. Theme selector (Switch selector) y pre-selector.
4. Regulator head.
5. Commuter or rupter (Diverter switch).

1. Activation and control closet: It is located in one of the transformer's side

exteriors and contains the control and maneuvering elements of the OLTC (engine start contacts, control push-buttons, electric engine, etc.)

2. **Transmission mechanism:** To change one tap to another, the OLTC is moved by a motorized driving mechanism through the vertical and horizontal transmission axes and angle redirection boxes. Any anomaly in the operation of any of the transmission mechanism can cause a deregulation, i.e. a situation in which the real position of the OLTC does not correspond to the indicated position in the control closet.
3. **Tap selector:** Conduces the load's current from the tap in use and selects the next tap. It may include a pre-selector or inverter that connects the main winding with the regulation winding in an additive or subtractive way allowing the duplication of the n positions.
4. **Head of the OLTC:** It has inside the energy accumulation mechanisms as well as the activation of the selector.
5. **Commuter or rupter:** It performs the commutation, i.e. passes from one tap to another without interrupting the service. It does so by using transitional resistances that limit the current when it operates short-circuiting two taps temporarily during change. The commuter is immersed in an oil deposit that is independent from the transformer's tank.



Figure 1. Basic structure of an OLTC.

3. Vibration Signals of an OLTC

The OLTC's vibration signal (Figure 2) while changing a tap have been registered with an accelerometer located in the head of the commuter calculating the vertical vibrations (axis y).

3.1 Signal treatment

The vibration signal has normalized and generated an envelope (Fig. 2) through the application of the Hilbert transform [3]. Posteriorly, the discrete Wavelet transform

(DWT) has been applied; a bi-orthogonal mother Wavelet 3.3 to find the main diagnosis indicators.

The DWT acts over the signal similarly to a bank of low-pass and high-pass filters decomposing the signal into an approximation function with the low-pass filter and a detailed signal with the high-pass filter which reduces the operation frequencies of the operator (Figure 3).

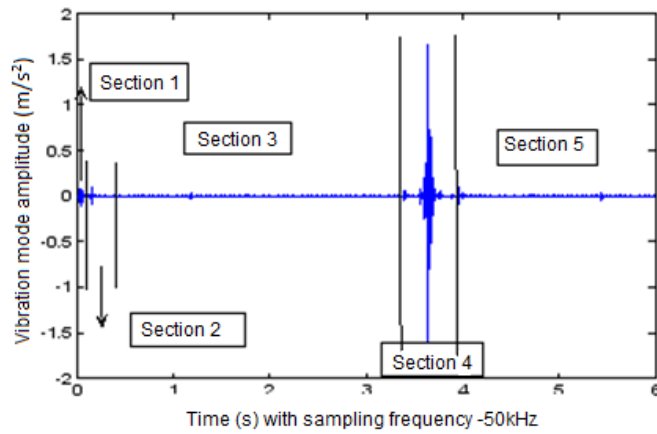


Figure 2. Vibration signal during a tap change.

1. The activation engine is turned on
2. Operation of auxiliary contacts of the control closet
3. Change of taps (connects the selected operation position)
4. Changes the commuter's contacts
5. The engine stops

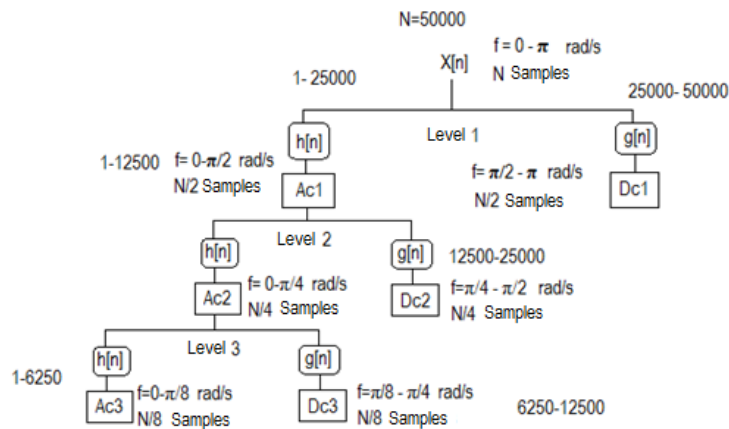


Figure 3. Wavelet decomposition.

By applying the reverse DWT and smoothing the signal with splines, the amplitude, the temporary location and the vibration pulses' frequency band are obtained [3] (Figure 4).

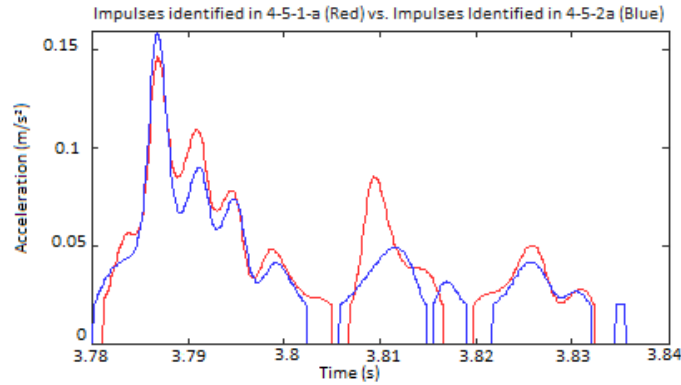


Figure 4. Impulses of the vibration signal.

Table 1. Location and amplitude of the vibration signal impulses.

<i>Impulses detected in signal 4-5-1 (red)</i>		
	Location (s)	Amplitude (m/s²)
Impulse 1	3,78684	0,1463021
Impulse 2	3,80944	0,085213
Impulse 3	3,8259	0,0500932
<i>Impulses detected in signal 4-5-2 (blue)</i>		
	Location (s)	Amplitude (m/s²)
Impulse 1	3,78678	0,1281312
Impulse 2	3,81164	0,0642687
Impulse 3	3,82576	0,0471563

For the detected impulses, their respective frequencies are obtained (Table 2) which are located in the 0 – 6250 Hz frequency range that corresponds to the third level of decomposition in the vibration signal.

Table 2. Frequencies of the vibration signal.

<i>Impulse</i>	<i>F₁</i>	<i>F₂</i>	<i>F₃</i>
1	552.427 Hz	3716.27 Hz	4419.417 Hz
2	602.426 Hz	3716.27 Hz	4052.62 Hz
3	444.839 Hz	3558 Hz	4052.62 Hz

Table 3 illustrates the frequency ranges that characterize the commuter after applying a set of 72 signals.

Table 3. Commuter frequencies through the use of DWT.

<i>Commuter frequencies through DWT</i>			
0-1500 Hz	1500 – 3000 Hz	3000-4500 Hz	4500-7000 Hz
390,625 Hz	1562.5 Hz	3125 Hz	5255.6 Hz
444.839 Hz	1858.136 Hz	3558 Hz	6250 Hz
552,427 Hz	2209.708 Hz	3716.272 Hz	
602.426 Hz	2627.801 Hz	4052.62	
781,25 Hz		4419.41 Hz	
929.068 Hz			
1104.854 Hz			
1313.9 Hz			

To corroborate the frequency results, the Fast Fourier transform (FFT) was applied obtaining the results shown in Figure 5 and Table 4.

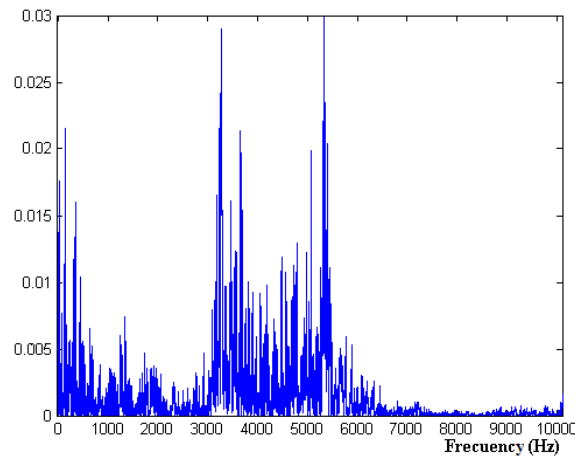


Figure 5. FFT of the signal during a tap change.

Table 4. Commuter frequencies through FFT.

<i>Commuter frequency intervals through FFT</i>				
0-500	3.100-3.700	4.400-4.800	4.900-5.100	5.200-5.500
0,2	3.179,3	4.480,8	4.978,6	5.255,6
24,3	3.240,8	4.561,5	5.073,0	5.300,8
136,1	3.267,3	4.735,2		5.308,4
144,5	3.283,3	4.781,3		5.317,2

Table 4. (Continued): Commuter frequencies through FFT.

149,5	3.455,0	4.788,9	5.337,2
298,8	3.472,0		5.372,0
323,0	3.535,5		5.394,5
335,3	3.568,3		5.402,0
347,2	3.653,1		5.410,3
442,7	3.683,3		5.455,5

Given that DWT is capable of determining the frequency range of the impulses without losing temporary resolution, the results obtained with this method were the ones used.

4. Commuter Modeling

The OLTC commutator has been modeled in SolidWorks™ and has been divided into three sections to facilitate its simulation and posterior analysis: Support cylinder (Figure 6), energy accumulator (Figure 7) and mobile contact disc (Figure 8). Screws and junction items were not considered due to their irrelevance in the simulation process.

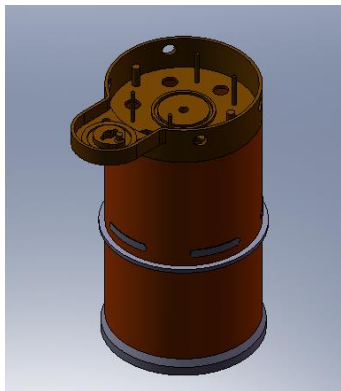


Figure 6. Support cylinder with OLTC head.

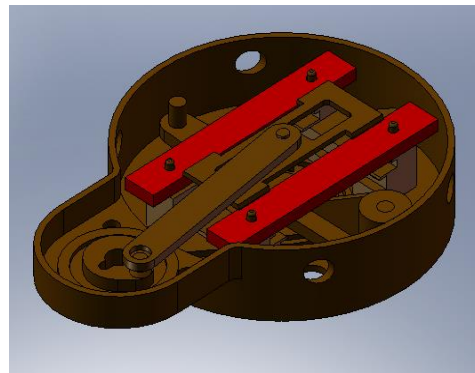


Figure 7. Energy accumulators.

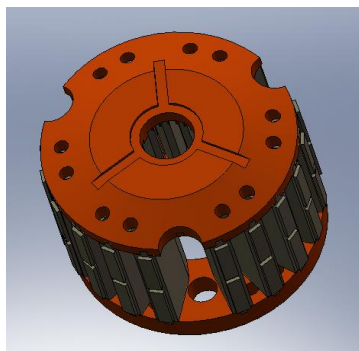


Figure 8. Disc for mobile contacts.

5. Simulation and Modal Analysis of the Commuter

With the purpose of determining the best surrounding condition to find the frequencies or vibration modes that the commuter is subjected to, two types of simulations were performed with the Algor™ software:

- a) Without fixating the set's bases (as a rigid body)
- b) Fixating the bases of the cylinder

The different vibration modes were compared to the frequencies for the scenarios of rigid body and fixed bases (Figure 9). It was concluded that frequencies coincide for different modes so that surrounding condition of the commuter is not a determining factor. Hence, the simulation process considers the bases as being fixed.

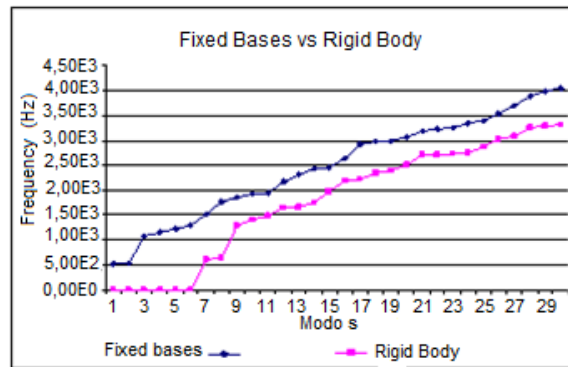


Figure 9. Natural frequencies for the contour conditions.

For the cylinder support, the energy accumulator and the disc for mobile contacts, 70, 70 and 150 simulation modes were carried out respectively. The results are shown in this section.

5.1 Support cylinder

Table 5, corresponding to Figure 10, shows the most significant modes (with the highest modal displacement in the y axis). These modes are the ones that pick up the most energy.

Table 5. The most significant modes for the cylinder.

<i>Support cylinder</i>				
Mode	Frequency (Hz)	Modal Mass (%)		
		X Axis	Y Axis	Z Axis
4	1,16E+03	0,92	2,36	1,07
6	1,30E+03	1,64	4,23	1,82
7	1,52E+03	0,02	38	0,02
12	2,17E+03	0,28	33,7	0,22
62	5,79E+03	0.03	2.30	0.04

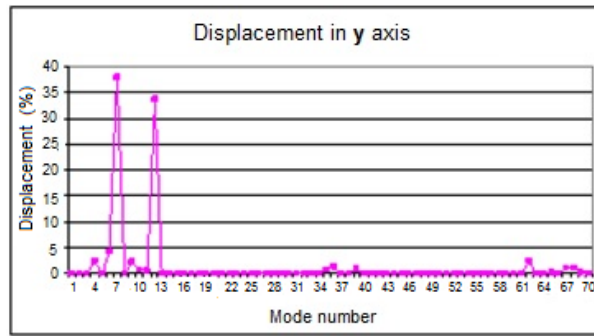


Figure 10. Percentage of mass displaced in the y axis.

In Figure 11 and 12 the modes 7 and 12 are shown which produce the highest displacements in the cylinder.

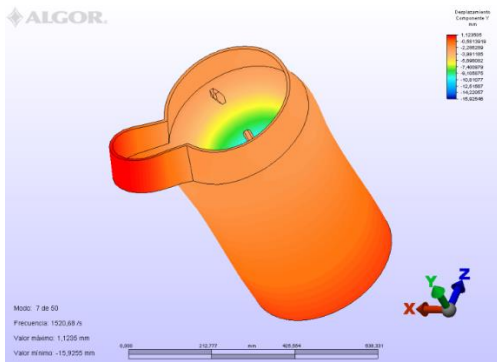


Figure 11. Modal mass displacement in mode 7.

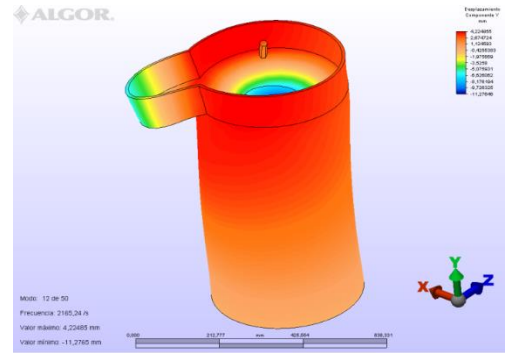


Figure 12. Modal mass displacement in mode 12.

5.2 Energy accumulator

The mode with the highest modal mass displacement is mode 1 (Table 6) as the other modes have an almost null displacement (Figure 13). The modal mass displacement is shown in Figure 14.

Table 6. Significant mode (mode 1) to the accumulator.

<i>Energy accumulator</i>				
Mode	Frequency (Hz)	Modal Mass (%)		
		Axis X	Axis Y	Axis Z
1	1,10E+03	0.00	5.34	0.04

5.3 Disc of mobile contacts

For this element, 100% of the modal displacement is almost reached between modes 60 and 73 (Figure 15), Table 7. The modal mass displacement of these modes is shown in Figure 16 and 17.

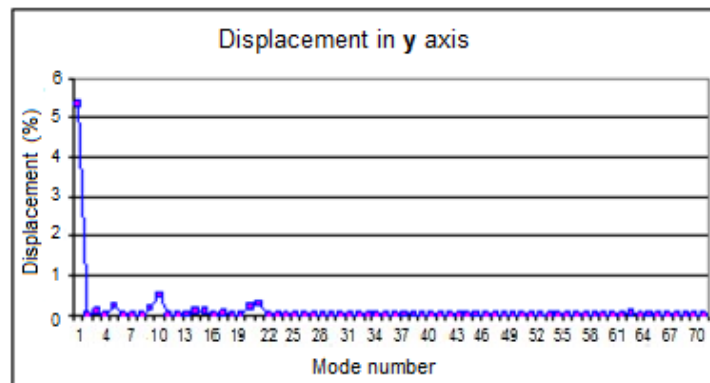


Figure 13. Percentage of mass displaced in the energy accumulator.

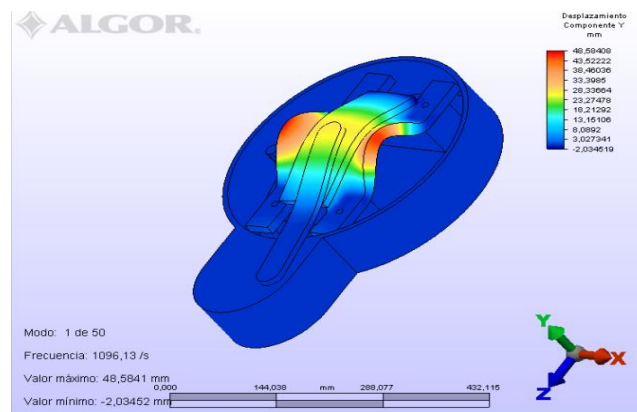


Figure 14. Modal mass displacement in mode 1 of the energy accumulator.

Table 7. Most significant modes for the disc of mobile contacts.

<i>Disc of mobile contacts</i>				
Mode	Frequency (Hz)	Modal Mass (%)		
		Axis X	Axis Y	Axis Z
60	2,12E+03	0.00	22.82	0.00
73	2,34E+03	0.00	73.27	0.00

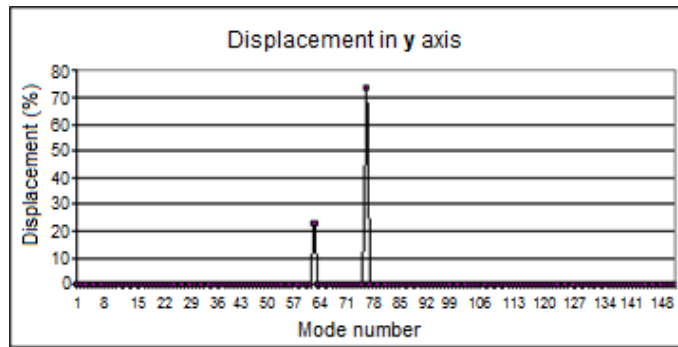


Figure 15. Percentage of mass displaced in the y axis.

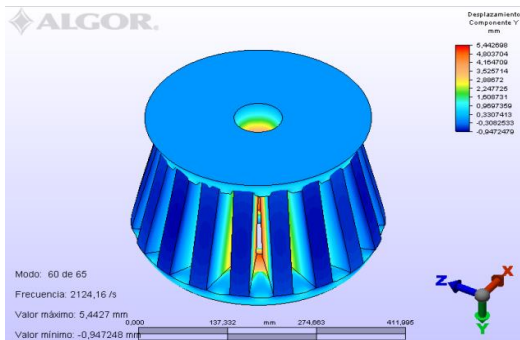


Figure 16. Modal mass displacement in mode 60.

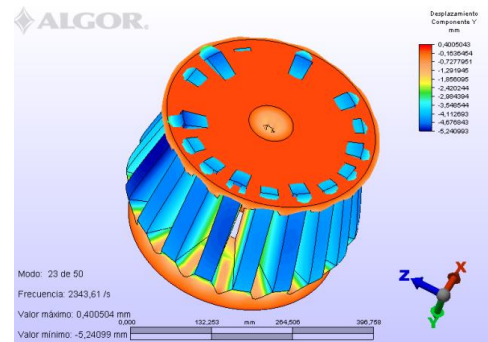


Figure 17. Modal mass displacement in mode 73.

6. Correlation: Operation Frequencies – Natural Frequencies

For the cylinder (Figure 18), the energy accumulator (Figure 19) and disc of mobile contacts (Figure 20), the natural frequencies that are closest to the OLTC operation frequencies were correlated. These natural frequencies do not represent a danger to the commuter since they have an almost null or null displacement.

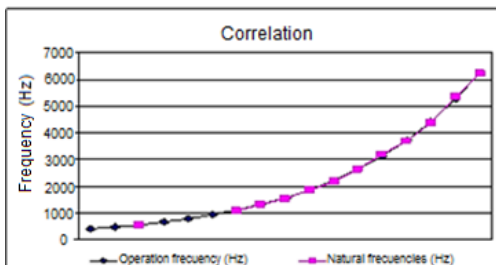


Figure 18. Correlation of frequencies for the support cylinder.

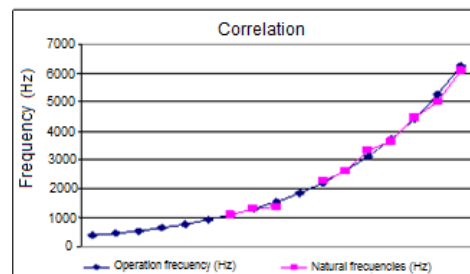


Figure 19. Correlation of frequencies for the energy accumulator.

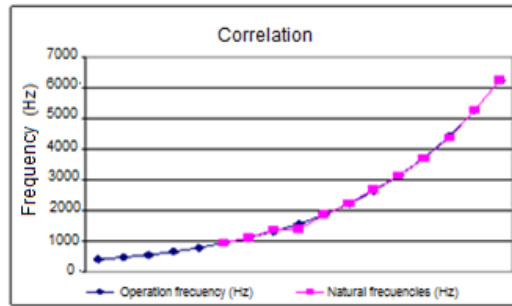


Figure 20. Correlation of frequencies for the disc of mobile contacts.

For the support cylinder (Figure 21, Table 7), the energy accumulator (Figure 22, Table 8) and the disc of mobile contacts (Figure 23, Table 9), the frequencies (operation frequencies versus natural frequencies) that produce large displacements in the commuter were correlated. If it operates during a certain time at this frequency, the resonance phenomenon can occur, as long as it has the same module and direction than the natural frequency.

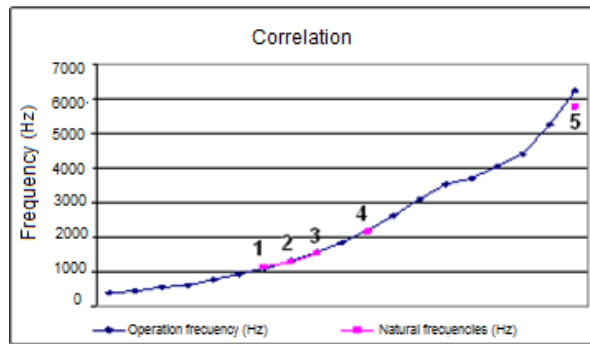


Figure 21. Correlation of frequencies for the support cylinder.

Table 7. Coinciding frequencies for the support cylinder.

	Operation Frequency (Hz)	Natural Frequency (Hz)	Frequency range (Hz)
1	1104.854	1160	0-1500
2	1313.9	1300	0-1500
3	1562.5	1520	1500-3000
4	2209.708	2170	1500-3000
5	6250	5790	4500-7000

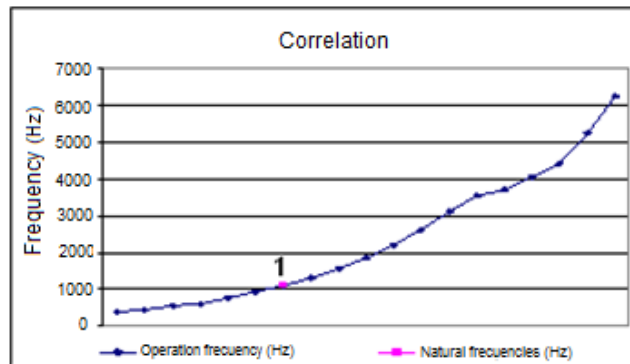


Figure 22. Correlation of frequencies for the energy accumulator

Table 8. Coinciding frequencies for the energy accumulator.

	Frecuencia de Operación(Hz)	Frecuencia Natural(Hz)	Rango Frecuencia(Hz)
1	1104.854	1100	0-1500 Hz

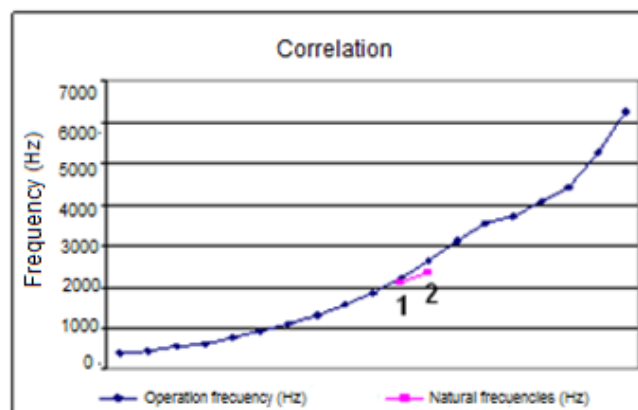


Figure 23. Correlation of frequencies for the disc of mobile contacts

Table 9. Coinciding frequencies for the disc of mobile contacts.

	F. Operation	F. Natural	Section
1	1104.854	1160	0-1500 Hz
2	1313.9	1300	0-1500 Hz

The natural frequency that is closest to the operation frequency is 1300 Hz, which belongs to mode 6 (1300 Hz, 4.23 %). The natural frequency of 1100 Hz (Table 8) corresponds to mode 1 with a 5.34% displacement. For the disc of mobile contacts,

natural frequencies are slightly away from the commuter's operation frequencies so there would be no danger if resonance occurred.

7. Conclusions

The frequency modes are not exactly obtained in a dynamic system so the OLTC's own vibration modes can be identified in the experimental vibration signal. Once the vibration modes' interval of frequencies is identified, a defect, an anomaly or malfunction can be detected when comparing two vibration signatures. The amplitude related to the frequency of one of the signatures increases or changes abruptly in its frequency interval.

To obtain the natural frequencies with finite element program, the adequate selection of the material's rigidity and mass are determining factors in the simulation process. At higher rigidity and lower mass, the resulting frequencies are more elevated.

The selected contour condition during the simulation is not a determining factor in the analysis since the obtained frequency values for different conditions are almost the same. The only variation was in the mode number containing that frequency which varies due to a different fixation of the pieces.

In the vibration modes whose natural frequencies are very close to the operation frequencies, a null displacement (or almost null) in the y axis was registered which would imply no energy accumulation, hence no danger for the functioning of the commuter's components.

For the commuter, the modes with large modal displacements where the natural frequency is close to the operation frequency had a frequency of 1300 Hz in mode 6 (4.23%) corresponding the support cylinder and 1100 Hz in mode 1 (5.34%) corresponding to the energy accumulator. During the tap change, the commuter could enter in resonance mode and produce a vibration state where it could not evacuate the stored energy and eventually collapse.

References

- [1] C. Bengtsson, Status and trends in transformer monitoring, *IEEE Trans. Power Delivery*, **11** (1996), 1379-1384. <https://doi.org/10.1109/61.517495>
- [2] CIGRE SC 12 WG 12.05, An international survey on failures in large power transformers in service, *Electra*, **88** (1983), 21-47.
- [3] E. Rivas, *Valoración del Estado de un OLTC Mediante Vibraciones: Análisis en Tiempo-Frecuencia*, M.S. Thesis, Dep. Electrical, Carlos III de Madrid Univ., Madrid, Spain, 2007.

Received: September 18, 2017; Published: November 1, 2017